

Article

Freezing Effect of Enhancing Tubes in a Freeze-Sealing Pipe Roof Method Based on the Unsteady-State Conjugate Heat Transfer Model

Shengjun Deng ^{1,2} , Dong Hu ¹, Siyuan She ³, Zequn Hong ⁴, Xiangdong Hu ⁵ and Feng Zhou ^{1,*}¹ Institute of Geotechnical Engineering, Nanjing Tech University, Nanjing 210009, China² Research Center of Coastal and Urban Geotechnical Engineering, Zhejiang University, Hangzhou 310058, China³ CapitaLand Investment Management, Shanghai 201114, China⁴ State Key Laboratory for Geomechanics and Deep Underground Engineering, School of Mechanics and Civil Engineering, China University of Mining and Technology, Xuzhou 221116, China⁵ Key Laboratory of Geotechnical and Engineering of Ministry of Education, Department of Geotechnical Engineering, Tongji University, Shanghai 200092, China

* Correspondence: zhoufeng@njtech.edu.cn; Tel.: +86-139-1384-4622

Abstract: The freeze-sealing pipe roof (FSPR) method was applied as an innovative construction technology to the Gongbei Tunnel of the Hong Kong–Zhuhai–Macau Bridge. A freezing scheme involving master freezing tubes, enhancing freezing tubes, and limiting freezing tubes is the key component of the freezing effect of the FSPR method during the construction process under various working conditions. This is related to whether the thickness and temperature of the frozen soil meet the design requirements under various complex working conditions, and it is also related to frost heave control and energy saving. Based on the unsteady-state conjugate heat transfer model, different freezing schemes of enhancing freezing tubes—that is, the shape, layout, operating duration, and heat preservation—were simulated to analyze the freezing effect, which can be measured by the thickness of frozen soil around the steel pipes and the average temperature of the frozen soil curtain. The results show that the greater the contact area between the enhancing tube and the inner wall of the steel pipe, the better the freezing effect, and that the semicircle enhancing freezing tube scheme is superior to the other three shapes of freezing tubes. The arrangement of enhancing freezing tubes far away from the excavation surface, without heat preservation measures, has a better freezing effect due to the function of the hollow pipe as a freezing pipe. Moreover, the enhancing freezing tube can be operated intermittently to control frost heave. Our research simulated the temperature fields of different media—such as steel pipes, frozen soil, and air—providing a design basis for similar projects, such as the combination of the pipe-roofing method and artificial freezing method.

Keywords: Gongbei Tunnel; freeze-sealing pipe roof method; heat transfer model; freezing scheme; enhancing freezing tube



Citation: Deng, S.; Hu, D.; She, S.; Hong, Z.; Hu, X.; Zhou, F. Freezing Effect of Enhancing Tubes in a Freeze-Sealing Pipe Roof Method Based on the Unsteady-State Conjugate Heat Transfer Model. *Buildings* **2022**, *12*, 1373. <https://doi.org/10.3390/buildings12091373>

Academic Editor: Suraparb Keawsawasvong

Received: 4 August 2022

Accepted: 30 August 2022

Published: 2 September 2022

Publisher's Note: MDPI stays neutral with regard to jurisdictional claims in published maps and institutional affiliations.



Copyright: © 2022 by the authors. Licensee MDPI, Basel, Switzerland. This article is an open access article distributed under the terms and conditions of the Creative Commons Attribution (CC BY) license (<https://creativecommons.org/licenses/by/4.0/>).

1. Introduction

The freeze-sealing pipe roof (FSPR) method, as an innovative pre-supporting method, was first applied in the Gongbei Tunnel of the Hong Kong–Zhuhai–Macao Bridge. The roofing pipes play the role of bearings, while the ground freezing mainly plays the role of sealing water. The freezing design of the FSPR method includes three types of freezing tubes—master freezing tubes, enhancing freezing tubes, and limiting freezing tubes—which is different from conventional freezing designs such as the one applied in the Berlin Metro Line 5 project [1]. Among these types of freezing tubes, enhancing freezing tubes are the most important to ensure the freezing effect. This is related to whether the thickness and temperature of the frozen soil meet the design requirements under various complex

working conditions, and it is also related to frost heave control and energy saving. However, there are only a few studies that specifically deal with enhancing freezing tubes.

To explore the effects of various design schemes of enhancing freezing tubes on the freezing effect, various research methods can be employed, such as analytical solutions, numerical simulations, model tests, and field tests. Since the freeze-sealing pipe roof method is a new type of tunnel pre-support method, it was first applied to the Gongbei Tunnel in China, and there have been few cases of its use in other countries. Therefore, the relevant technical standards and specifications were mostly formulated in China, and the research results have mainly been reported by Chinese scholars. Temperature is one of the important indicators to evaluate the freezing effect. In terms of analytical solutions, a new typical freezing temperature model of the FSPR method was proposed, with the freezing tubes arranged inside jacking pipes, and then an analytical solution to the steady-state temperature field was obtained by transforming the circular boundary condition to a linear boundary condition via conformal mapping and superposition methods [2]. Then, the FSPR model based on the Gongbei Tunnel was proposed, considering the operation of limiting freezing tubes, and the analytical solution of the steady-state temperature field was first investigated using the superposition method and boundary separation method of the Laplace equation [3]. However, the analytical solution can only solve the simplified model of the FSPR method, which concerns regularly symmetric objects far from the actual project. Model tests can achieve studies of similar scale and size. A physical model test on temperature field of a large-scale FSPR structure was conducted to validate the freezing effect [4]. Similar mechanical model tests of the FSPR method based on two and three steel pipes were also carried out to optimize the design of suitable freezing temperatures from the perspective of water-sealing performance [5]. The influence of thermal disturbance of FSPR structures during construction on the freezing effect was explored by model tests [6]. Compared with model tests, field tests can effectively reduce the size effect. A field test on the active freezing scheme of the FSPR method was conducted to analyze the freezing effect under different freezing modes [7]. The freezing effect and optimal freezing scheme of the FSPR method in different phases was also explored [8]. However, field tests are time-consuming and overly expensive, so it is difficult to conduct all tests that consider various parameters. Therefore, numerical simulation is a relatively good method, and the freezing effect can be visually observed through the simulation results. Temperature simulation of the FSPR method can be carried out during the active and maintained freezing phase, which is similar to the work described in [9,10]. The influence of operating and stop duration of enhancing freezing tubes on the freezing effect of the FSPR method was analyzed by numerical simulation [11]. Combined with the monitoring method of the excavation surface, the construction safety factor can be further improved [12,13].

In the above numerical simulation model, frozen soil is regarded as the only heat transfer medium, and the temperature boundary is directly assigned to the outer surface of the steel pipe. However, the heat conduction process in the real project is designed with three media: steel pipes, frozen soil, and air. Therefore, this research concerns the numerical simulation of a specific shape of enhancing freezing tubes and the heat conduction between different media, i.e., steel pipes, frozen soil, and air. An optimized design proposal requires the comparison of different shapes of enhancing freezing tubes through numerical simulation, and it is necessary to consider unsteady-state conjugate heat transfer between various media. The research on enhancing freezing tubes is crucial to the reliability of water sealing and frost heave control of the FSPR method. This study takes the Gongbei Tunnel of the Hong Kong–Zhuhai–Macao Bridge as the engineering background, and explores the freezing effect of enhancing freezing tubes with different design shapes, layout, operating duration, and heat preservation measures, based on the unsteady-state conjugate heat transfer theory.

2. Engineering Background

The Gongbei Tunnel is a key link of the Hong Kong–Zhuhai–Macao Bridge. The layout of the FSPR method is shown in Figure 1. During construction, 36 steel pipes with a diameter of $\Phi 1620$ mm and thickness of 20 mm were jacked; among them, the odd-numbered steel jacking pipes were full of concrete, while the even-numbered jacking pipes were hollow. The two types of pipes were arranged alternately, with a spacing of 357 mm. The two types of jacking pipes were arranged in a staggered manner inside and outside; the height difference of the circle center was 300 mm, and the buried depth of the tunnel was 4~5 m.

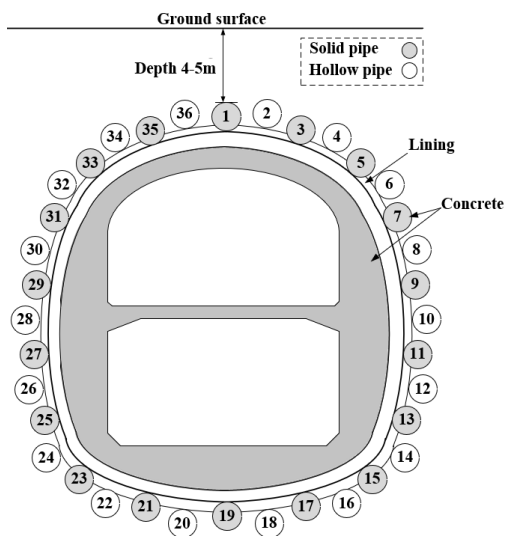


Figure 1. Layout scheme of the freeze-sealing pipe roof method.

The layout of the freeze-sealing pipe roof method in the Gongbei Tunnel includes three types of freezing tubes: master freezing tubes with a diameter of 133 mm and thickness of 4 mm, limiting freezing tubes with a diameter of 133 mm and thickness of 4 mm, and enhancing freezing tubes with a diameter of 159 mm and thickness of 4.5 mm; the layout of the enhancing freezing tubes is shown in Figure 2.

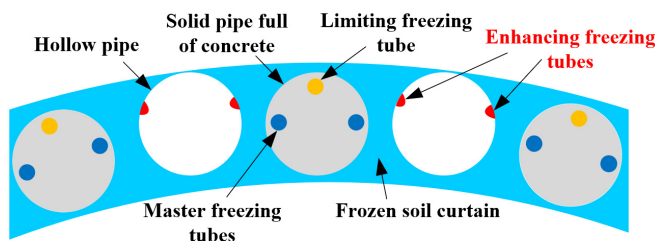


Figure 2. Layout of the freezing tubes in the pipe-roofing.

Among the freezing tubes, the function of the master freezing tubes is to freeze the soil between the jacking pipes. The limiting freezing tubes mainly limit the thickness of the frozen soil to control frost heave by increasing the temperature. There are two main functions of enhancing freezing tubes: the first is to strengthen the freezing effect; the second is to resist the hydration heat during the pouring of concrete to maintain the thickness of the FSPR structure. Therefore, further research on the appearance, layout, and freezing scheme of enhancing freezing tubes is necessary to ensure the freezing effect and frost heave control.

3. Numerical Model

3.1. Assumptions and Computational Model

The Gongbei Tunnel is a typical engineering case of the FSPR method, and is used as a case study in this paper. To establish an efficient computational model, the typical parts of the FSPR structure are taken as the computational model, as shown in Figure 3. The size of the model is 11 m × 1.977 m. For the unsteady-state conjugate heat conduction model, the left and right sides and the lower part of the model are the soil, which can be regarded as the second temperature boundary condition. The upper part of the model is the ground surface, which can be regarded as the third boundary condition [14,15]. Inside the model, the freezing tube as a cold source can be regarded as the first temperature boundary condition, and the temperature of the brine flowing into the main tube is used as the boundary temperature [16]. The steel pipe is a conjugate heat transfer surface [17]. In this computational model, the strong coupling integral computational method is selected, and the general control equation is used to find a global solution. Therefore, the initial values of the temperature field, velocity field, and pressure field need to be given for the whole region. For the initial value of the velocity field, both the solid domain and fluid domain are recorded as 0 m/s; for the initial pressure distribution, the fluid and solid domains are denoted as 1 atm. The upper boundary that represents the ground surface is regarded as the convective heat transfer boundary. The heat flux q in the lower boundary is 0.4 W/m², as expressed by Equation (1). The left and right boundaries are the adiabatic boundaries.

$$q = \lambda \frac{\partial T}{\partial y} \quad (1)$$

where λ is the thermal conductivity of the soil, and $\frac{\partial T}{\partial y}$ is the geothermal gradient, with a value of 0.03 °C/m.

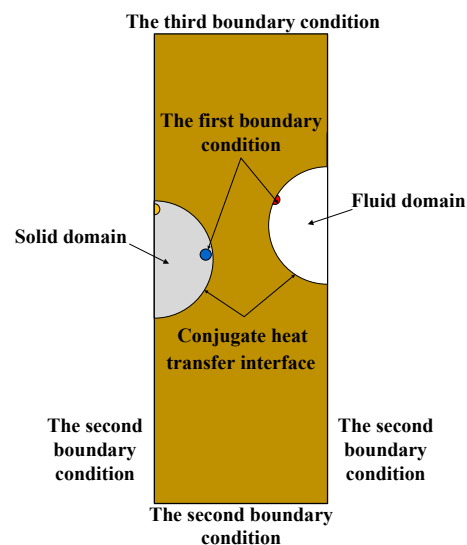


Figure 3. Computational model of the FSPR method based on unsteady-state conjugate heat transfer.

3.2. Governing Equation of Unsteady-State Conjugate Heat Transfer Model

Ground freezing is an unsteady-state heat transfer process with complex phase transition. In the solidification process of pure substances such as water, solidification occurs at a single temperature, and the solid phase and liquid phase are separated by a clear moving interface. However, the soil freezing occurs in a larger temperature range, and there is a separation of the solid and liquid phases by moving regions of two phases in the process [18]. The phase transition problem is mathematically strongly nonlinear, meaning that the governing equation is linear, but the position of the two-phase interface must always be determined, and the energy conservation condition of the interface is nonlinear. It is not

possible to use the superposition principle of solutions. Therefore, most of these problems are treated by numerical simulation methods [19]. When using numerical methods to solve phase transition problems, there are generally two methods to deal with the moving boundary in the process of phase transition: The first focuses on the solution of the phase transition interface. After determining the interface position, the temperature distributions in the solid and liquid regions are solved. The second method is to assume the problem as a single-phase nonlinear heat conduction problem, determine the temperature or enthalpy distribution in the whole solution region, and then determine the position to reach the phase transition temperature as the phase transition interface [20–22]. The second method is convenient and practical, and is more suitable for the soil phase transformation process, which has no clear interface. For the second method, the sensible heat capacity method is used. Assuming that the physical properties of the solid and liquid phases are spatially invariant, ignoring the possible natural convection in the liquid phase, the conjugate heat transfer interface between soil and air is the steel pipe. The sensible heat capacity method takes temperature as the function to be solved, without introducing the concept of enthalpy, and establishes a unified energy equation for the whole region. For the treatment of phase transition, the specific heat is expressed in the form of equivalent specific heat [23,24]. For convenience of explanation and comparison with the enthalpy method, the equivalent specific heat of phase transition that occurs at a given temperature T_m is as expressed in Equation (2):

$$\tilde{c}(T) = c(T) + L\delta(T - T_m);$$

$$c(T) = \begin{cases} c_s(T) & T < T_m \\ c_l(T) & T > T_m \end{cases}; \delta(T - T_m) = \begin{cases} 1 & T = T_m \\ 0 & T \neq T_m \end{cases} \quad (2)$$

where $\delta(T - T_m)$ is a Dirac function and, thus, has a heat capacity model as shown in Equation (3):

$$\rho\tilde{c}\frac{\partial T}{\partial t} = \text{div}(\lambda \text{grad } T) \quad (3)$$

References [25,26] proved the equivalence between Equation (3) and the commonly used equations describing the phase transition problem.

For the phase transition that occurs in the temperature range near $T_m(T_m \pm \Delta T)$, the influence of T should be taken into account when constructing the equivalent specific heat. The expression \tilde{c} should be expressed as shown in Equation (4):

$$\tilde{c}(T) = \begin{cases} c_s(T) & T < (T_m - \Delta T) \\ c_l(T) & T > (T_m + \Delta T) \end{cases};$$

$$\int_{T_m - \Delta T}^{T_m + \Delta T} \tilde{c}(T) dT = L + \int_{T_m - \Delta T}^{T_m} c_s(T) dT + \int_{T_m}^{T_m + \Delta T} c_l(T) dT \quad (4)$$

When the specific heat and coefficient of thermal conductivity of the solid phase and liquid phase are constant, Equation (5) can be obtained:

$$\lambda = \begin{cases} \lambda_s & T < (T_m - \Delta T) \\ \lambda_s + \frac{\lambda_l - \lambda_s}{2\Delta T} [T - (T_m - \Delta T)] & (T_m - \Delta T) \leq T \leq (T_m + \Delta T) \\ \lambda_l & T > (T_m + \Delta T) \end{cases};$$

$$\tilde{c}(T) = \begin{cases} c_s & T < (T_m - \Delta T) \\ \frac{L}{2\Delta T} + \frac{c_s + c_l}{2} & (T_m - \Delta T) \leq T \leq (T_m + \Delta T) \\ c_l & T > (T_m + \Delta T) \end{cases} \quad (5)$$

References [18,27,28] note that the phase change of water in frozen soil can be divided into three regions:

- (1) Severe phase transition zone: when the temperature in this zone changes by 1 °C, the variation in unfrozen water content is greater than or equal to 1%;

- (2) Transition zone: when the temperature in this zone changes by 1 °C, the variation in unfrozen water content is between 0.1% and 1%;
- (2) Frozen zone: when the temperature in this zone decreases by 1 °C, the amount of the water phase becoming ice is less than 0.1%.

Accordingly, when the sensible heat capacity method is used to deal with the phase change problem of the soil freezing process, the change in the unfrozen water in the soil should be divided into at least three sections according to the experimental data—a violent phase change zone, transition zone, and frozen solid zone—and then the phase change should be treated with the equivalent specific heat in each section.

Similar to references [29,30], the specific heat of the soil region is as shown in Equation (6):

$$c(T) = \begin{cases} c_f & T < T_b \\ c_f + \frac{c_u - c_f}{T_a - T_b} (T - T_b) + \frac{L}{(1+w)} \frac{\partial w_i}{\partial T} & T_a \leq T \leq T_b \\ c_u & T > T_a \end{cases} \quad (6)$$

where c_u, c_f represent the specific heat of unfrozen soil and frozen soil, respectively (unit: J/(kg·K)); L is the latent heat of the phase change of water; w and w_i are the total water content and ice content of the frozen soil, respectively; and T_a and T_b are the upper and lower boundary temperatures of the frozen soil's phase transition zone, respectively.

In the hollow pipe, when the air pressure is low and the temperature is high, the air can be treated as an ideal gas [31]. The air in the fluid domain can also be regarded as a compressed fluid and a viscous fluid. At this time, the continuity equation and motion equation (Navier–Stokes equation) are changed. Considering the causes of fluid movement, the flow state of air can be assumed to be laminar flow. The continuous condition of heat flux can also be treated according to laminar flow in the conjugate heat transfer interface [32].

According to the above assumptions, the general strong coupling control equations of the computational model can be obtained, containing the energy equation, ideal gas state equation, continuity equation, and motion equation.

The energy equation can be expressed with Equation (7):

$$\rho c \frac{\partial T}{\partial t} = \text{div}(\lambda \text{grad } T) + \Phi \quad (7)$$

The ideal gas state equation can be expressed with Equation (8):

$$p = \rho RT \quad (8)$$

The continuity equation can be expressed with Equation (9):

$$\frac{D\rho}{Dt} + \rho \text{div } \mathbf{v} = 0 \quad (9)$$

The motion equation can be expressed with Equation (10):

$$\rho \frac{D\mathbf{v}}{Dt} = \mathbf{F} - \text{grad } p + \text{div}(2\mu\mathbf{S}) - \frac{2}{3} \text{grad}(\mu \text{div } \mathbf{v}) \quad (10)$$

where ρ represents the fluid density, c represents the specific heat shown in Equation (6), \mathbf{v} represents the velocity vector, λ represents the thermal conductivity, T represents the temperature, t represents time, μ represents the coefficient of viscosity, Φ represents the intensity of the internal heat source, and R represents the gas constant, $R = R_0/M$.

3.3. Model Parameter

The properties of the typical soil layer in Gongbei Tunnel are shown in Table 1. The thermal conductivity of the soil and air is shown in Table 2. The air viscosity is shown in

Table 3. The specific heat at constant pressure of air is shown in Table 4. The properties of steel and concrete are shown in Table 5.

Table 1. Properties of typical soil layers in Gongbei Tunnel.

Soil Layer Number	Lithology	Moisture Content w (%)	Density ρ (kg/m ³)	Dry Density ρ_d (kg/m ³)
①	Artificial fill	16.05	1660	1470
③-3	Pebble sand	13.54	2000	1760
④-3	Muddy silty clay	47.6	1820	1230
⑤-1	Silty clay	26.37	2010	1590
⑤-2	Fine sand	18.25	1950	1650
⑤-3	Muddy silty clay	38.27	1880	1360
⑥-2	Medium sand	17.92	2020	1720
⑦-1	Gravel clay	31.98	1890	1430
⑧-1	Completely decomposed granite	17.31	2040	1740
⑧-2	Highly weathered granite	19.65	1980	1650

Table 2. Thermal conductivity of soil and air (W/(m·K)).

Material Names	Thermal Conductivity at Different Temperatures						
	−30 °C	−20 °C	−10 °C	0 °C	10 °C	20 °C	30 °C
①-Artificial fill	/	1.962	1.690	1.511	1.398	1.109	/
③-3 Pebble sand	/	1.925	1.758	1.538	1.217	1.066	/
④-3 Muddy silty clay	/	2.047	1.772	1.614	1.485	1.206	/
⑤-2 Fine sand	/	2.019	1.775	1.719	1.497	1.266	/
⑤-3 Muddy silty clay	/	1.994	1.893	1.643	1.402	1.344	/
⑦-1 Gravel clay	/	2.030	1.790	1.623	1.442	1.319	/
Air	0.022	0.0228	0.0236	0.0244	0.0251	0.0259	0.0267

Table 3. Air viscosity (μ Pa·s).

−40 °C	−20 °C	0 °C	10 °C	20 °C	30 °C
15.60	16.83	17.09	17.59	18.08	18.56

Table 4. Specific heat at constant pressure of air (J/(kg·K)).

−30 °C	−20 °C	−10 °C	0 °C	10 °C	20 °C	30 °C
1011	1009	1009	1010	1012	1013	1014

Table 5. Properties of steel and concrete.

Material	Density (kg/m ³)	Thermal Conductivity (W/(kg·K))	Specific Heat (J/(kg·K))
Steel	7850	44.7	459.8
Concrete	2344	1.835	419.8

3.4. The Shape of the Enhancing Freezing Tubes

Research on the shape of enhancing freezing tubes, which has a significant effect on the freezing effect, is lacking. This is the basis of the follow-up work in this paper. Since the air flow in the hollow pipes has a great impact on the enhancing freezing tubes [33], enhancing freezing tubes with different cross-sectional shapes were compared to improve the heat transfer efficiency. The enhancing freezing tubes of different shapes—such as circular, crescent, groove, and semicircular—are shown in Figure 4. To amplify and compare the computational results of the freezing effect, these four types of enhancing freezing tubes were given the same cross-sectional area and tripled to 0.047 m².

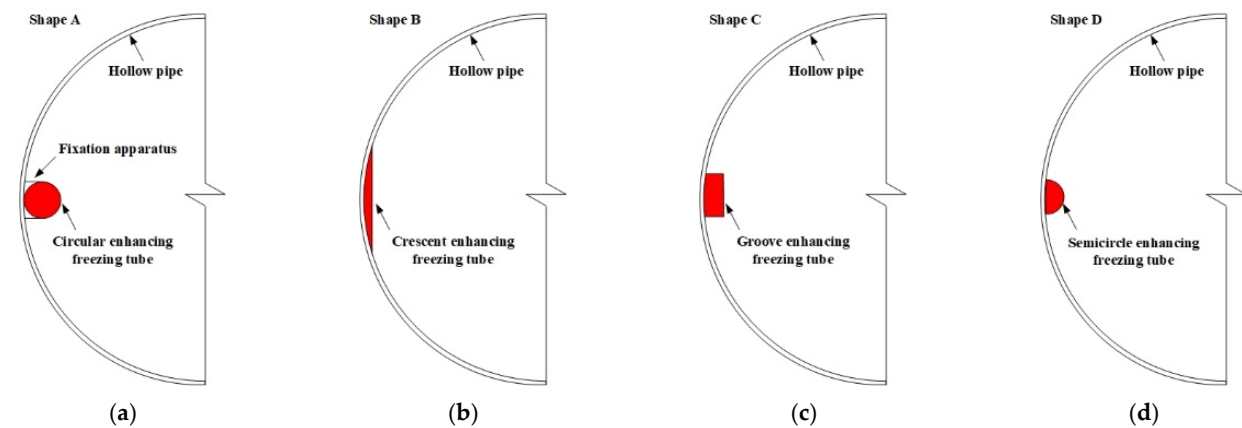


Figure 4. Cross-sectional shapes of enhancing freezing tubes: circular tube (a); crescent tube (b); groove tube (c); semicircular tube (d).

The temperature cloud graphs of the enhancing tubes with different shapes over the course of 30 days during the active freezing phase are shown in Figure 5. After 30 days of active freezing, the frozen soil curtain formed between the two pipes based on the different shapes of the enhancing tubes. The frozen soil curtain of Shape A and Shape D was more uniform, while the non-uniformity of the frozen soil curtain of Shape B and Shape C was greater than that of Shape A and Shape D, which may lead to frost heaving.

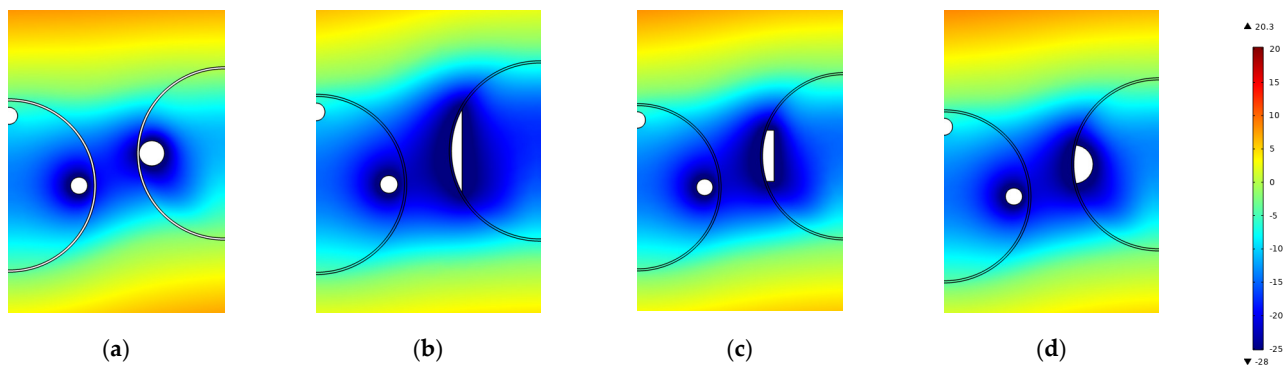


Figure 5. Temperature cloud graphs of enhancing freezing tubes with different shapes (freezing for 30 days): Shape A (a), Shape B (b), Shape C (c), Shape D (d).

As shown in Figure 6, the average temperature of the hollow pipe with a circular tube was the highest, while that of the hollow pipe with a crescent tube was the lowest. If the contact area between the enhancing freezing tube and the inner surface of the hollow pipe is increased as much as possible, the cooling capacity of the enhancing freezing tubes can be effectively and quickly transferred to the soil. The average temperature of the circular enhancing freezing tubes of Shape A was the highest; the freezing effect of these tubes was weaker than that of Shape D due to the small contact surface between the enhancing freezing tubes and the steel pipe. Therefore, the scheme of Shape A should be abandoned.

Although the average temperature of the enhancing freezing tubes of Shape B and Shape C was lower, the non-uniformity of their frozen soil curtain thickness was relatively greater. Taking the area below $-10\text{ }^{\circ}\text{C}$ as the strength of the frozen soil curtain [34,35], it can be concluded from Table 6 that the thickness of the frozen soil curtain with Shape B was the thickest, and had the greatest degree of unevenness. Uneven frost heaving is detrimental to the pipeline and the surrounding environment [36,37]. To avoid uneven frost heaving, Shape B should be abandoned. The thickness of the frozen soil curtain with Shape C and Shape D was similar, but the degree of unevenness in the thickness of Shape D was far less than that of Shape C. Therefore, the semicircular enhancing freezing tube is the

best scheme in terms of the freezing effect and the degree of unevenness in the thickness of the frozen soil curtain.

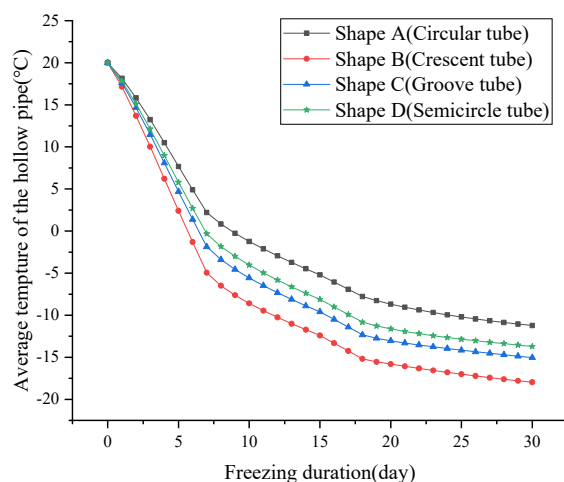


Figure 6. Average temperature of the hollow pipes.

Table 6. Comparison of the freezing effects of enhancing tubes with different shapes.

Active Freezing for 30 Days	Shape A		Shape B		Shape C		Shape D	
	Left Side	Right Side						
Thickness of frozen soil curtain (m)	1.076	0.938	1.274	1.477	1.225	1.288	1.193	1.195
Differentials (m)	0.138		0.203		0.063		0.002	
Thickness unevenness degree	12.825%		15.934%		5.143%		1.676%	

Remark: The thickness unevenness degree is the ratio of the differentials and the thickness of the frozen soil curtain on the left side.

3.5. Calculation Scheme

Research on the layout of enhancing freezing tubes is the most important factor in the FSPR freezing scheme. The layout of the enhancing freezing tubes has a great influence on the freezing effect and time, which is the most concerned part in construction sites. To understand the influence of the layout, operating duration, and heat preservation measures of the semicircular enhancing freezing tubes on the freezing effect, three different simulation schemes were set up, as shown in Figure 7. The initial temperature of the model was set at 20 °C, and the surface boundary was set as the third boundary condition, with a surface heat transfer coefficient of 15 W/(kg·K).

The layout of the enhancing freezing tubes has great influence on the freezing effect [38]. A freezing scheme of enhancing freezing tubes in two different positions was considered, as shown in Figure 5a. The enhancing freezing tubes were arranged far from or near to the excavation side with an angle of 15°, recorded as Scheme A and Scheme B, respectively. The master freezing tubes and enhancing freezing tubes were operated from the beginning to the end of the freezing process.

The operating duration of the enhancing freezing tubes was also set as a simulation scheme involving weather, to make the enhancing freezing tubes work and maintain an active freezing duration of 60 days, recorded as Scheme C and Scheme D. The master freezing tubes continued working during this period.

Most of the engineering literature on the use of the artificial ground freezing method posits that air convection has a great influence on the freezing temperature field [39]. The air convection interface should be insulated to limit and reduce the loss of cooling capacity caused by air convection, so as to concentrate the cooling capacity on the formation and development of frozen soil. Fortunately, each section of the hollow jacking pipes has thermal insulation treatment in the longitudinal direction, and the air in the jacking pipe

did not undergo directly convect with the atmosphere during the freezing construction of the Gongbei Tunnel. The convective heat transfer in the limited space has limited heat dissipation; even this kind of air convection can homogenize the cold capacity of the enhancing freezing tubes, and make the hollow pipes play the role of “freezing pipe”, which is beneficial to the freezing effect. Therefore, whether the strengthening of heat preservation measures is beneficial to the freezing effect must be discussed through simulation comparison. The simulation scheme is shown in Figure 7b, where the models with and without heat preservation measures are recorded as Scheme E and Scheme F, respectively.

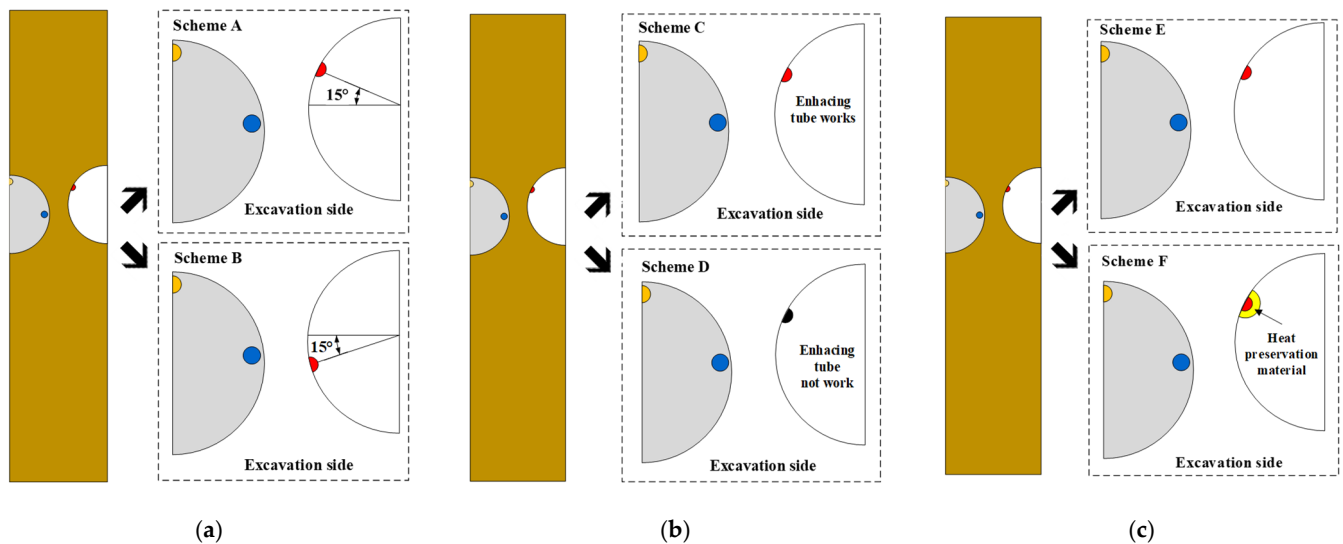


Figure 7. Calculation scheme of enhancing freezing tubes: layout angle (a), operating duration (b), heat preservation measures (c).

According to the engineering scheme [40], polyurethane foam was selected as the heat preservation material. The thickness of the heat preservation material was set to 0.03 m based on construction experience [41,42]. The thermal conductivity of the heat preservation material was set to 0.04 W/(kg·K), the density was 34 kg/m³, and the specific heat was 2016 J/(kg·K).

4. Results and Analysis

4.1. The Layout of the Enhancing Freezing Tubes

Figure 8a,b show the temperature distribution in different layouts of enhancing freezing tubes over different durations. As the change in temperature causes the air density to change, the cooler air sinks to the bottom of the pipe, and the hotter air floats to the crown of the pipe. This air flow further aggravates the change in the temperature field, and cyclically reciprocates until it reaches an equilibrium state. The results show that the air convection velocity field under the two freezing schemes reached a state of distribution equilibrium after 30 days of active freezing. The arrangement of the enhancing freezing tubes in Scheme A is more conducive to the air flow. Therefore, Scheme A is better than Scheme B in terms of distribution range and flow rate, and can effectively ensure the full flow of air through the entire hollow pipe.

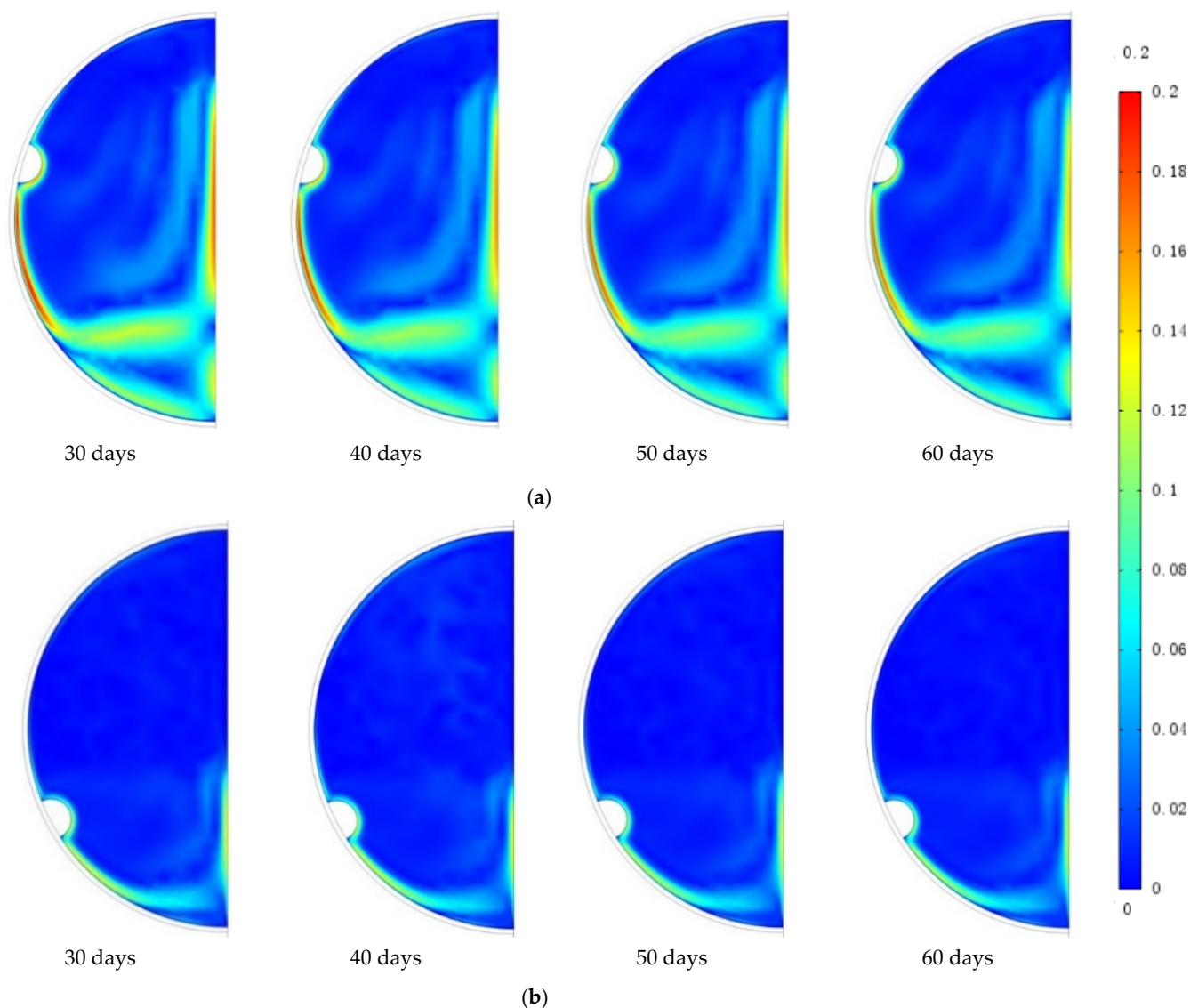


Figure 8. Temperature distribution cloud graphs of the different layouts of the enhancing freezing tubes: Scheme A (a); Scheme B (b).

When comparing the enhancing freezing tube schemes, the thickness of the frozen soil curtain is the most important criterion, including the thickness of frozen soil between the pipes and the thickness of frozen soil at the central axis of the steel pipe. Figure 9 shows the changes in the thickness of the frozen soil curtain of Scheme A and Scheme B over time.

Figure 10 shows that the frozen soil curtain formed after 7 days of the freezing process. For Scheme A, the frozen soil curtain reached the thickness of 2.0 m required by the design requirements after 33 days of active freezing, while it needed to freeze for 38 days to reach 2 m in Scheme B. Additionally, the thickness of the frozen soil curtain at the central axis of the steel pipe in Scheme A was also greater than that of Scheme B. Therefore, Scheme A is better than Scheme B. Figure 11 shows the thickness of the frozen soil at the central axis of the steel pipe, including the upper section and the bottom section.

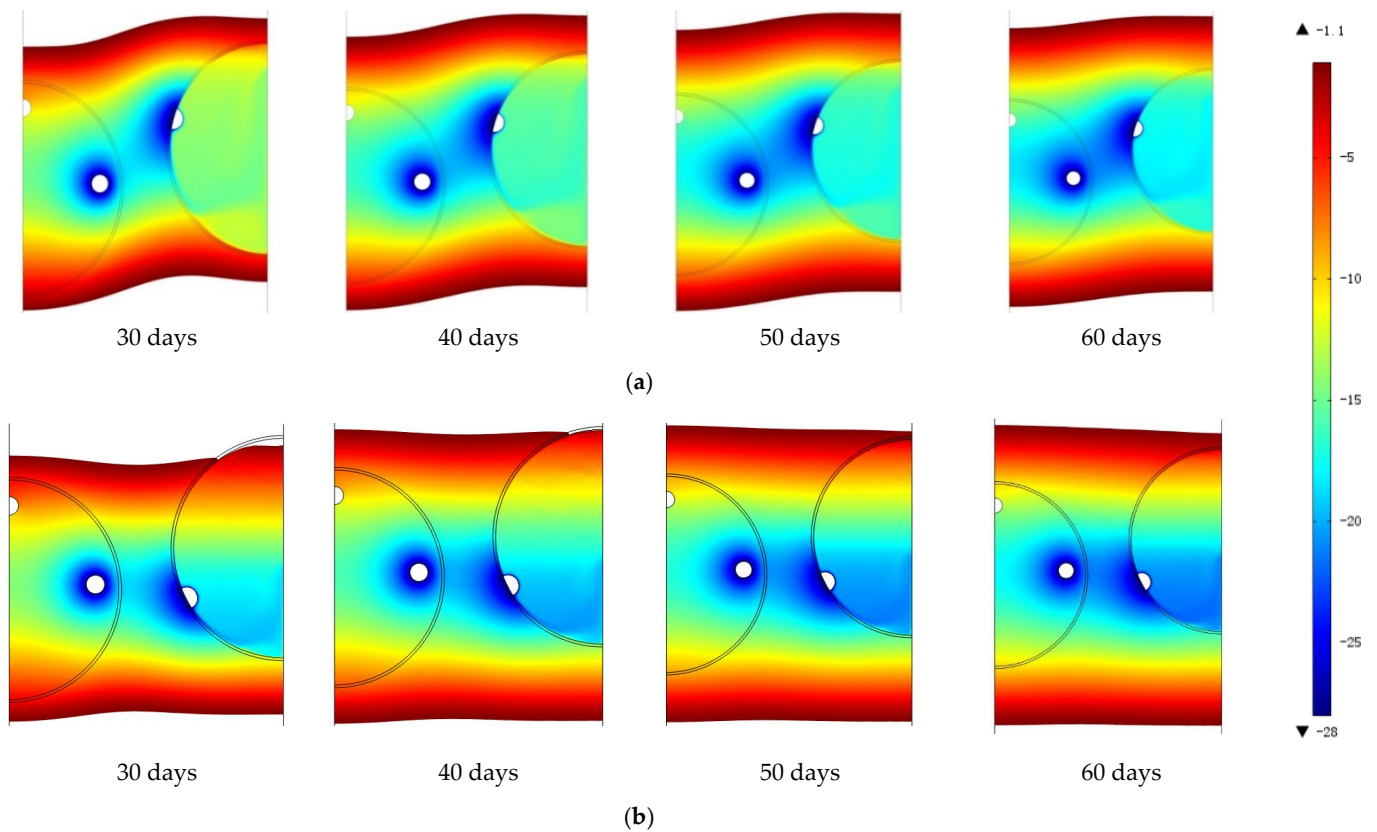


Figure 9. Temperature cloud graphs of the different layouts of the enhancing freezing tubes: Scheme A (a); Scheme B (b).

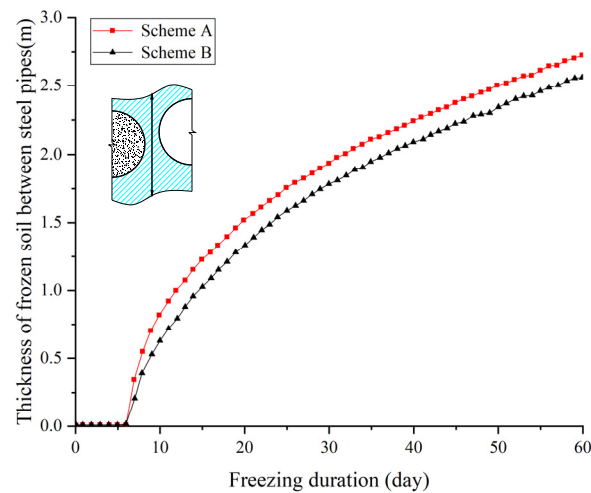


Figure 10. The thickness of the frozen soil between the pipes.

In summary, the layout of the enhancing freezing tubes should be fully considered in promoting the full flow of air in the hollow pipe. The basic law of air flow is that the colder air sinks to the bottom while the warmer air floats to the top. For the pipe jacking on the upper part of the FSPR structure, the layout of the enhancing freezing tubes should be slightly outside the excavation surface. The specific position can be fine-tuned according to the steel jacking process. Generally, it can be located at about 15 degrees counterclockwise to the horizontal radius of the hollow jacking pipe, as shown in Figure 7a.

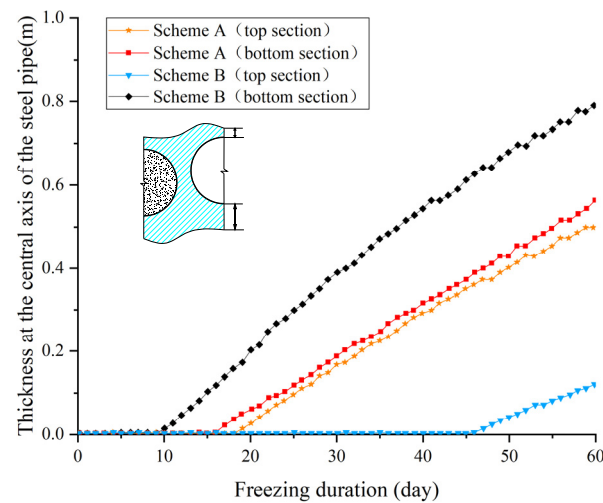


Figure 11. The thickness of the frozen soil at the central axis of the steel pipe.

4.2. The Operating Duration of the Enhancing Freezing Tubes

According to the above results, Scheme A is the best plan. The operating duration of the enhancing freezing tubes was also set as a simulation scheme, involving weather, to make the enhancing freezing tubes maintain an active freezing duration of 60 days, recorded as Scheme C and Scheme D. The master freezing tubes continued working during this period.

Figure 12 shows the temperature cloud graphs for different operating durations. After 60 days of freezing, the thickness of the frozen soil curtain in Scheme D still struggled to reach the thickness required by the design.

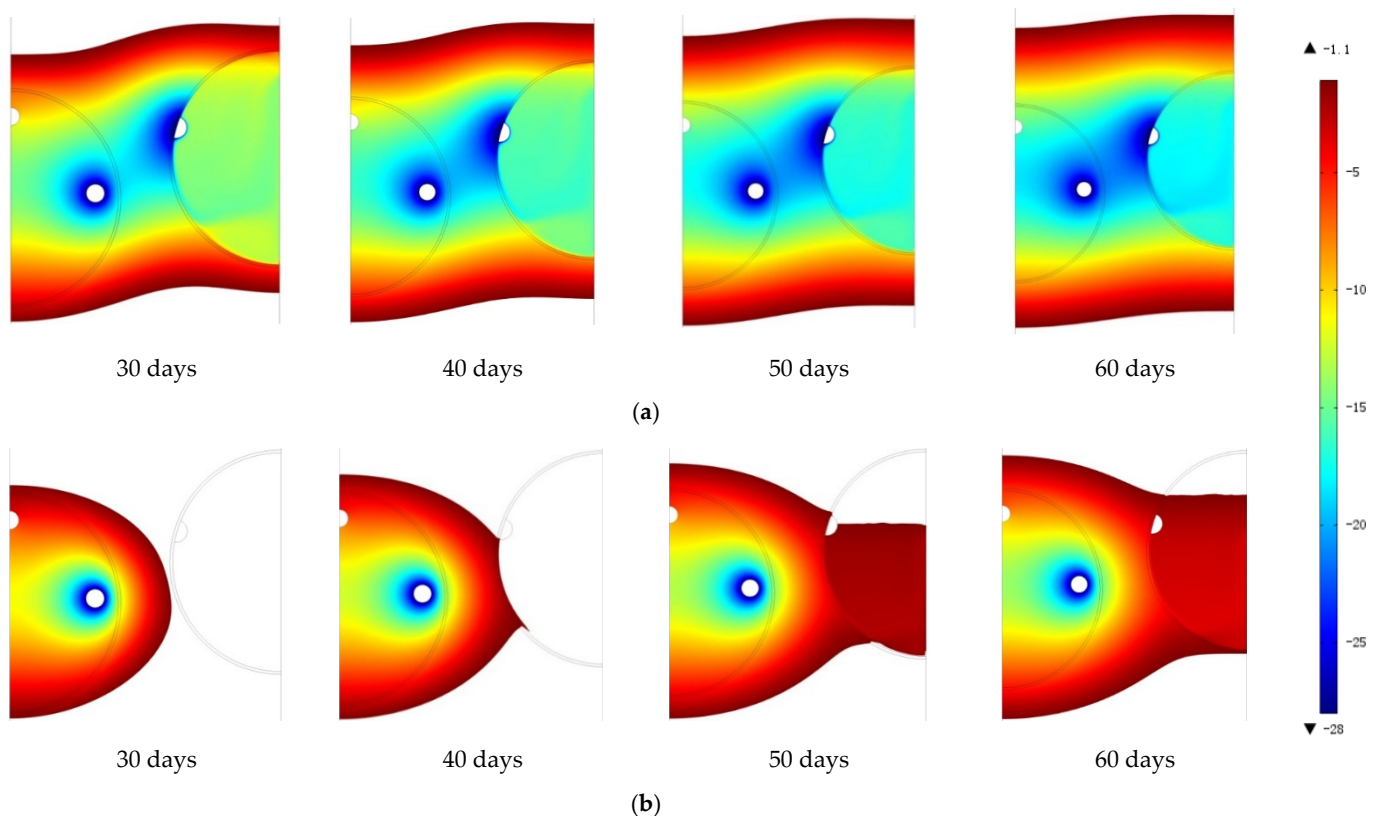


Figure 12. Temperature cloud graphs of the different operating durations of the enhancing freezing tubes: Scheme C (a); Scheme D (b).

Figure 13 compares the development conditions of the frozen soil curtains under the two schemes. In Scheme C, the frozen soil curtain intersected on the 6th day of freezing, and reached a thickness of 2 m in about 32 days. However, the frozen soil curtain intersected after 17 days of freezing in Scheme D, and the thickness of frozen soil reached only 1.75 m after 60 days of freezing, as shown in Figure 13. Moreover, the average temperature showed a similar trend, struggling to meet the design requirements in Scheme D, as shown in Figure 14. Therefore, Scheme C is better than Scheme D.

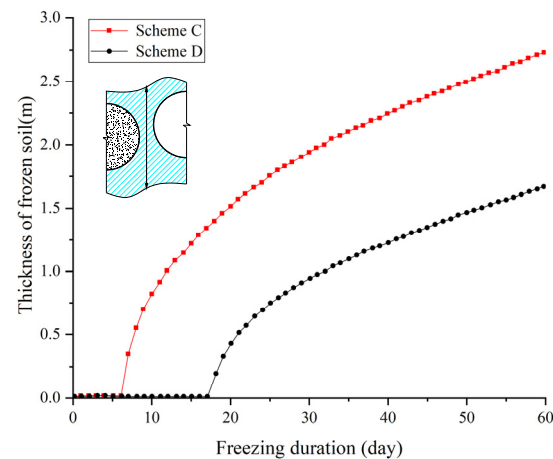


Figure 13. The thickness of the frozen soil between the pipes.

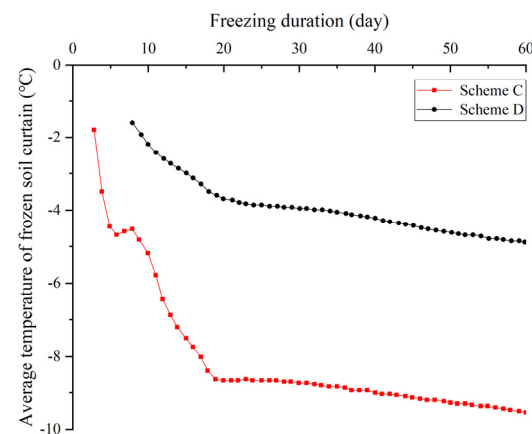


Figure 14. The average temperature of the frozen soil curtains.

Taking the construction period of Gongbei Tunnel into account, the master freezing tubes and the enhancing freezing tubes should be operated at the same time during the construction. However, this may cause the frozen soil area in the longitudinal partial area to be too large during construction. Therefore, from the perspective of controlling frost heave, it may be necessary to carry out intermittent operating and closing treatments for the enhancing freezing tubes. In summary, Scheme C, in which the two types of freezing tubes are working at the same time, should be the recommended scheme.

4.3. The Heat Preservation Measures of the Enhancing Freezing Tubes

In the construction of the freezing section of the pipe curtain in Gongbei Tunnel, the hollow pipe had heat preservation measures in the longitudinal direction. The air convection was not in an open state connected with the atmosphere, and the heat dissipation caused by convection heat transfer in limited space was objectively limited. More importantly, the air convection in the hollow pipe can homogenize the cooling capacity of the enhancing freezing tubes, so that the pipe can play the role of freezing. Therefore, whether

the strengthening of heat preservation measures is beneficial to the freezing effect needs to be studied through simulation comparison.

Figures 15 and 16 show that Scheme E (without heat preservation measures) has a better freezing effect than Scheme F (with heat preservation measures). Because the heat preservation measures promote the suppression of the cold source in the hollow pipe, the thickness of the frozen soil in Scheme E is obviously greater than that in Scheme F, including the thickness of the frozen soil between the steel pipes and that at the central axis of the steel pipe, as shown in Figures 15 and 16, respectively. Therefore, Scheme E is more effective.

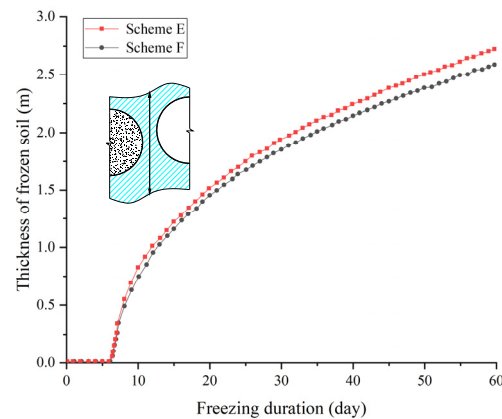


Figure 15. The thickness of the frozen soil between the steel pipes.

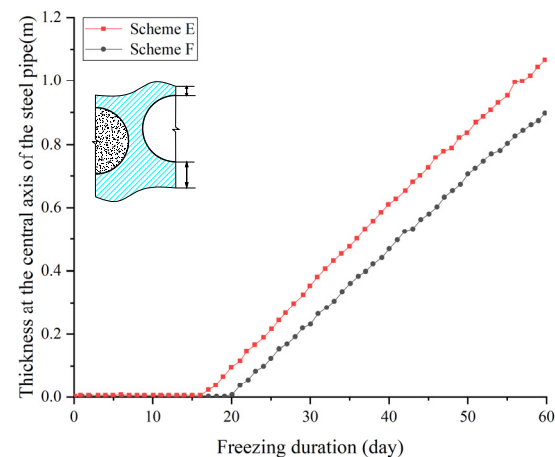


Figure 16. Thickness of the frozen soil at the central axis of the steel pipe.

The average temperature of the frozen soil curtain in Scheme E was 5 °C lower than that in Scheme F, as shown in Figure 17. The state of active freezing for 40 days is shown in Figure 18. In Scheme F, the value of the air velocity field was slightly smaller than that of Scheme E, due to the addition of heat preservation measures. According to the above findings, the heat preservation material makes the temperature in the hollow pipe decrease slowly, and the hollow pipe does not fully play the role of a large freezing pipe, reducing the freezing efficiency.

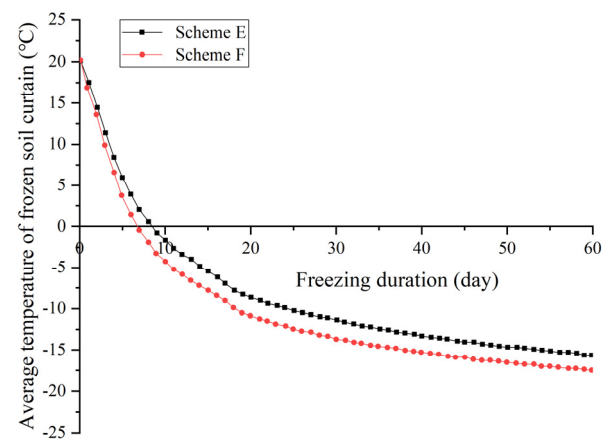


Figure 17. Average temperature of the frozen soil curtains.

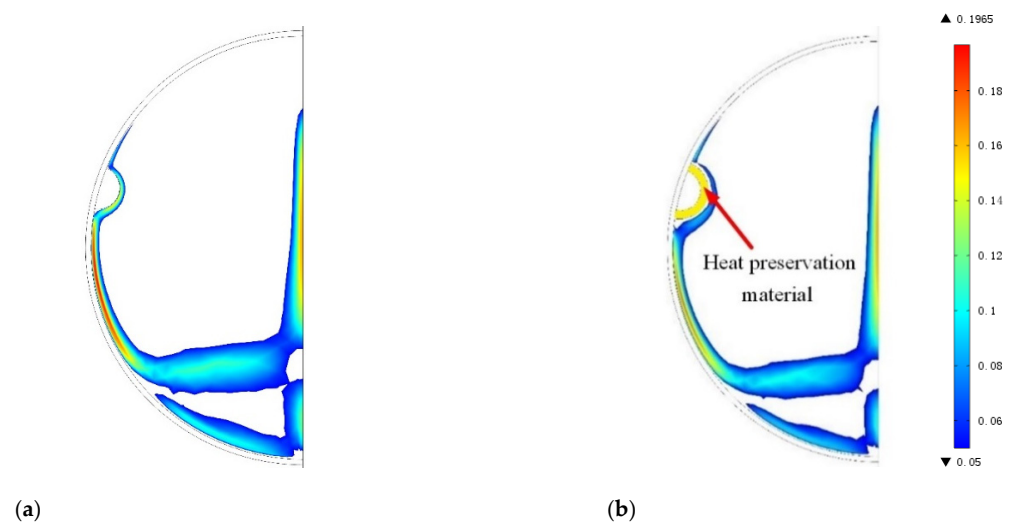


Figure 18. Velocity cloud diagrams of the enhancing freezing tubes with or without the heat preservation measures (active freezing for 40 days): Scheme E (a); Scheme F (b).

Based on the above analysis, it can be determined that the heat preservation measures of the enhancing freezing tubes cannot significantly reduce the loss of cooling capacity of the tubes due to air convection heat transfer, but the freezing effect is significantly weakened after the heat preservation of the enhancing freezing tubes. Therefore, there is no need to install heat preservation measures during the freezing process.

5. Conclusions

In this paper, based on the unsteady conjugate heat transfer model, the temperature field of the FSPR project including three heat transfer media—steel pipe, frozen soil, and air—was successfully simulated, and the simulation accuracy can be used for engineering guidance. Then, the simulation and analysis of the layout, operating duration, and heat preservation of the enhancing freezing tubes in Gongbei Tunnel were carried out; the following conclusions were obtained:

- (1) The greater the contact area between the enhancing freezing tube and the inner wall of the steel pipe, the better the freezing effect. Considering both the freezing effect and frost heave control, the semicircular enhancing freezing tube scheme is superior to the other three shapes of freezing tubes.
- (2) The enhancing freezing tubes arranged far away from the excavation surface (Scheme B) have a better freezing effect.

- (3) The freezing efficiency is the highest when the enhancing freezing tubes and the master freezing tubes are operated at the same time (Scheme C), but the enhancing freezing tubes can be operated and closed intermittently according to the working conditions to control frost heave.
- (4) The effect of the heat preservation measures of the enhancing freezing tubes is not obvious, but it does affect the cooling capacity of the air in the hollow pipe which, in turn, affects the function of the hollow pipe as a freezing pipe, thereby affecting the freezing effect. It is recommended not to use heat preservation measures (Scheme E).

Author Contributions: Conceptualization, S.D.; methodology, S.D.; formal analysis, D.H. and S.S.; investigation, Z.H.; resources, X.H.; data curation, S.D.; writing—original draft preparation, Z.H.; writing—review and editing, S.D. and D.H.; visualization, Z.H.; supervision, S.S.; project administration, F.Z.; funding acquisition, F.Z. and S.D. All authors have read and agreed to the published version of the manuscript.

Funding: This work is supported by the financial support from National Natural Science Foundation of China (No. 52008208 and 51778287), Natural Science Foundation of Jiangsu Province (No. BK20200707), The Natural Science Foundation of the Jiangsu Higher Education Institutions of China (No. 20KJB560029), China Postdoctoral Science Foundation (No. 2020M671670), Key Laboratory of Soft Soils and Geoenvironmental Engineering (Zhejiang University), Ministry of Education (No. 2020P04), the support above is gratefully acknowledged.

Institutional Review Board Statement: Not applicable.

Informed Consent Statement: Not applicable.

Data Availability Statement: The data used to support the findings of this study are available from the authors upon request.

Acknowledgments: The authors wishes to give special thanks to Rayhan Howlader for the language editing work.

Conflicts of Interest: The authors declare that they have no conflict of interest to report regarding the present study.

References

1. Jörg, S.; Paul, E.; Josef, S. Metro Line U5 In Berlin—Design Challenges Due To Complex Geotechnical Conditions/U-Bahnlinie U5 In Berlin—Besondere Herausforderungen Für Die Planung Aufgrund Der Komplexen Geotechnischen Gegebenheiten. *Geomech. Und Tunnelbau* **2013**, *6*, 487–493. [[CrossRef](#)]
2. Hu, X.; Hong, Z.; Fang, T. Analytical Solution to Steady-State Temperature Field with Typical Freezing Tube Layout Employed in Freeze-Sealing Pipe Roof Method. *Tunn. Undergr. Space Technol.* **2018**, *79*, 336–345. [[CrossRef](#)]
3. Hong, Z.; Hu, X.; Fang, T. Analytical Solution to Steady-State Temperature Field of Freeze-Sealing Pipe Roof Applied to Gongbei Tunnel Considering Operation of Limiting Tubes. *Tunn. Undergr. Space Technol.* **2020**, *105*, 103571. [[CrossRef](#)]
4. Hu, Q.; Shi, R.; Hu, Y.; Cai, Q.; Qu, M.; Zhao, W.; He, L. Method to Evaluate the Safety of Tunnels through Steeply Inclined Strata in Cold Regions Based on the Sidewall Frost Heave Model. *J. Perform. Constr. Facil.* **2018**, *32*, 04018030. [[CrossRef](#)]
5. Hu, X.; Fang, T.; Chen, J.; Ren, H.; Guo, W. A Large-Scale Physical Model Test on Frozen Status in Freeze-Sealing Pipe Roof Method for Tunnel Construction. *Tunn. Undergr. Space Technol.* **2018**, *72*, 55–63. [[CrossRef](#)]
6. Li, Z.; Wang, W.; Hu, X. Research on Influence of Construction Thermal Disturbance on the Freezing-Sealing Pipe Roof. *Tumu Gongcheng Xuebao/China Civ. Eng. J.* **2015**, *48*, 374–379.
7. Ren, H.; Hu, X.; Hong, Z.; Zhang, J. Experimental Study on Active Freezing Scheme of Freeze-Sealing Pipe Roof Used in Ultra-Shallow Buried Tunnels. *Yantu Gongcheng Xuebao/Chin. J. Geotech. Eng.* **2019**, *41*, 320–328. [[CrossRef](#)]
8. Hu, X.; Deng, S.; Wang, Y. Test Investigation on Mechanical Behavior of Steel Pipe-Frozen Soil Composite Structure Based on Freeze-Sealing Pipe Roof Applied to Gongbei Tunnel. *Tunn. Undergr. Space Technol.* **2018**, *79*, 346–355. [[CrossRef](#)]
9. Kostina, A.; Zhelnin, M.; Plekhov, O.; Agutin, K.A. THM-Coupled Numerical Analysis of Temperature and Groundwater Level in-Situ Measurements in Artificial Ground Freezing. *Frat. Ed. Integr. Strutt.* **2022**, *16*, 1–19. [[CrossRef](#)]
10. Tounsi, H.; Rouabhi, A.; Tijani, M.; Guerin, F. Thermo-Hydro-Mechanical Modeling of Artificial Ground Freezing: Application in Mining Engineering. *Rock Mech. Rock Eng.* **2019**, *52*, 3889–3907. [[CrossRef](#)]
11. Li, J.; Li, Z.; Hu, X. Analysis on Water Sealing Effect of Freezing-Sealing Pipe Roof Method. *Dixia Kongjian Yu Gongcheng Xuebao/Chin. J. Undergr. Space Eng.* **2015**, *11*, 751–758.
12. Chen, J.; Zhang, D.; Huang, H.; Shadabfar, M.; Zhou, M.; Yang, T. Image-Based Segmentation and Quantification of Weak Interlayers in Rock Tunnel Face via Deep Learning. *Autom. Constr.* **2020**, *120*, 103371. [[CrossRef](#)]

13. Chen, J.; Zhou, M.; Huang, H.; Zhang, D.; Peng, Z. Automated Extraction and Evaluation of Fracture Trace Maps from Rock Tunnel Face Images via Deep Learning. *Int. J. Rock Mech. Min. Sci.* **2021**, *142*, 104745. [[CrossRef](#)]
14. Zueter, A.F.; Xu, M.; Alzoubi, M.A.; Sasmito, A.P. Development of Conjugate Reduced-Order Models for Selective Artificial Ground Freezing: Thermal and Computational Analysis. *Appl. Therm. Eng.* **2021**, *190*, 116782. [[CrossRef](#)]
15. Vitel, M.; Rouabhi, A.; Tijani, M.; Guerin, F. Modeling Heat Transfer between a Freeze Pipe and the Surrounding Ground during Artificial Ground Freezing Activities. *Comput. Geotechnics* **2015**, *63*, 99–111. [[CrossRef](#)]
16. Qi, Y.; Zhang, J.; Yang, H.; Song, Y. Application of Artificial Ground Freezing Technology in Modern Urban Underground Engineering. *Adv. Mater. Sci. Eng.* **2020**, *2020*, 1619721. [[CrossRef](#)]
17. Alzoubi, M.A.; Nie-Rouquette, A.; Sasmito, A.P. Conjugate Heat Transfer in Artificial Ground Freezing Using Enthalpy-Porosity Method: Experiments and Model Validation. *Int. J. Heat Mass Transfer.* **2018**, *126*, 740–752. [[CrossRef](#)]
18. Kozłowski, T. A Comprehensive Method of Determining the Soil Unfrozen Water Curves 2. Stages of the Phase Change Process in Frozen Soil-Water System. *Cold Reg. Sci. Technol.* **2003**, *36*, 81–92. [[CrossRef](#)]
19. Singh, S.; Bhargava, R. Numerical Simulation of a Phase Transition Problem with Natural Convection Using Hybrid FEM/EFGM Technique. *Int. J. Numer. Methods Heat Fluid Flow.* **2015**, *25*, 570–592. [[CrossRef](#)]
20. Bellur, K.; Médiçi, E.F.; Hermanson, J.C.; Choi, C.K.; Allen, J.S. Determining Solid-Fluid Interface Temperature Distribution during Phase Change of Cryogenic Propellants Using Transient Thermal Modeling. *Cryogenics* **2018**, *91*, 103–111. [[CrossRef](#)]
21. Frolov, D. Calculating Scheme of Ground Freezing Depth on the Basis of Data on Seasonal Snowfall Deposition, Snow Cover Accumulation and Temperature Variation. In Proceedings of the 9th International Conference on Computational Information Technologies for Environmental Sciences, Moscow, Russia, 27 May–6 June 2019; IPO Publishing Ltd.: Beijing, China, 2019; Volume 386.
22. Park, J.; Yoon, H.-K.; Kim, J. Effect of Water Distribution Patterns on the Activation Energy of Unsaturated Soils during Phase Transformation. *Vadose Zone J.* **2021**, *20*, e20170. [[CrossRef](#)]
23. Yao, M.; Chait, A. An Alternative Formulation of the Apparent Heat-Capacity Method for Phase-Change Problems. *Numer Heat Transf. B-Fundam.* **1993**, *24*, 279–300. [[CrossRef](#)]
24. Bonacina, C.; Comini, G.; Fasano, A.; Primicerio, M. Numerical Solution of Phase-Change Problems. *Int. J. Heat Mass Transf.* **1973**, *16*, 1825–1832. [[CrossRef](#)]
25. Pepper, D.W. Computational Heat Transfer Using The Method of Second Moments. *Numer. Heat Transf. Part. B Fundam.* **2002**, *42*, 189–201. [[CrossRef](#)]
26. Bronfenbrener, L. A Non-Instantaneous Kinetic Model for Freezing in Porous Media. *Chem. Eng. Processing: Process. Intensifi.* **2008**, *47*, 1631–1646. [[CrossRef](#)]
27. Stuurup, J.C.; Van der Zee, S.E.A.T.M.; Voss, C.I.; French, H.K. Simulating Water and Heat Transport with Freezing and Cryosuction in Unsaturated Soil: Comparing an Empirical, Semi-Empirical and Physically-Based Approach. *Adv. Water Resour.* **2021**, *149*, 103846. [[CrossRef](#)]
28. Kebria, M.M.; Na, S.; Yu, F. An Algorithmic Framework for Computational Estimation of Soil Freezing Characteristic Curves. *Int. J. Numer. Anal. Methods Geomech.* **2022**, *46*, 1544–1565. [[CrossRef](#)]
29. Lee, R.; Chiou, W. Finite-Element Analysis of Phase-Change Problems Using Multilevel Techniques. *Numer. Heat Transf.* **1995**, *27*, 277–290. [[CrossRef](#)]
30. Hromadka, T.V.; Guymon, G.L.; Berg, R.L. Some Approaches to Modeling Phase Change in Freezing Solids. *Cold Reg. Sci. Technol.* **1981**, *4*, 137–145. [[CrossRef](#)]
31. Ryzhkov, S.V.; Kuzenov, V.V. Analysis of the Ideal Gas Flow over Body of Basic Geometrical Shape. *Int. J. Heat Mass Transf.* **2019**, *132*, 587–592. [[CrossRef](#)]
32. Tiwari, N.; Moharana, M.K. Effect of Conjugate Heat Transfer in Single-Phase Laminar Flow through Partially Heated Microtubes. *Sadhana Acad. Proc. Eng. Sci.* **2021**, *46*, 28. [[CrossRef](#)]
33. Sugawara, M.; Tago, M. Freezing of Water in a Closed Vertical Tube Cooled by Air Flow. *Int. J. Heat Mass Transf.* **2019**, *133*, 800–811. [[CrossRef](#)]
34. De Guzman, E.M.B.; Stafford, D.; Alfaro, M.C.; Doré, G.; Arenson, L.U. Large-Scale Direct Shear Testing of Compacted Frozen Soil under Freezing and Thawing Conditions. *Cold Reg. Sci. Technol.* **2018**, *151*, 138–147. [[CrossRef](#)]
35. Wang, J.; Nishimura, S.; Tokoro, T. Laboratory Study and Interpretation of Mechanical Behavior of Frozen Clay through State Concept. *Soils Found.* **2017**, *57*, 194–210. [[CrossRef](#)]
36. Palmer, A.C.; Williams, P.J. Frost Heave and Pipeline Upheaval Buckling. *Can. Geotech. J.* **2003**, *40*, 1033–1038. [[CrossRef](#)]
37. Peterson, R.A. Assessing the Role of Differential Frost Heave in the Origin of Non-Sorted Circles. *Quat. Res.* **2011**, *75*, 325–333. [[CrossRef](#)]
38. Zueter, A.F.; Madiseh, A.G.; Hassani, F.P.; Sasmito, A.P. Effect of Freeze Pipe Eccentricity in Selective Artificial Ground Freezing Applications. *J. Therm. Sci. Eng. Appl.* **2021**, *14*, 1884–2023. [[CrossRef](#)]
39. Tabilo, E.J.; Moraga, N.O. Improved Water Freezing with Baffles Attached to a Freezing Tunnel: Mathematical Modeling and Numerical Simulation by a Conjugate Finite Volume Model. *Int. J. Refrig.* **2021**, *128*, 177–185. [[CrossRef](#)]
40. Gusyachkin, A.M.; Sabitov, L.S.; Khakimova, A.M.; Hayrullin, A.R. Effects of Moisture Content on Thermal Conductivity of Thermal Insulation Materials. *IOP Conf. Ser. Mater. Sci. Eng.* **2019**, *570*, 012029. [[CrossRef](#)]

41. Birsan, D.C.; Scutelnicu, E.; Visan, D. Modeling of Heat Transfer in Pipeline Steel Joint Performed by Submerged Double-Arc Welding Procedure. *Adv. Mater. Res.* **2013**, *814*, 33–40. [[CrossRef](#)]
42. Sanchez, N.; Güngör, Ö.E.; Liebeherr, M.; Ilić, N. Development of X80M Line Pipe Steel for Spiral Welded Pipes With Low Temperature Toughness and Excellent Weldability. In Proceedings of the 2014 10th International Pipeline Conference, Risk and Reliability, Calgary, AB, Canada, 29 September–3 October 2014; pp. 1–11. [[CrossRef](#)]